



1 **Evaluation of a low-cost optical particle counter (Alphasense OPC-N2)** 2 **for ambient air monitoring**

3
 4 Leigh R. Crilley¹, Marvin Shaw², Ryan Pound², Louisa J. Kramer¹, Robin Price³, Stuart
 5 Young², Alastair C Lewis², Francis D. Pope^{1*}

6
 7 ¹*School of Geography, Earth and Environmental Sciences, University of Birmingham,*
 8 *Birmingham, United Kingdom, B15 2TT.*

9 ²*National Centre for Atmospheric Science, Wolfson Atmospheric Chemistry Laboratories,*
 10 *University of York, York, United Kingdom, YO10 5DD.*

11 ³*Birmingham Open Media (BOM), 1 Dudley Street, Birmingham, B5 4EG.*

12 **Corresponding author – f.pope@bham.ac.uk*

13 **Abstract**

14 A fast growing area of research is the development of low-cost sensors for measuring air
 15 pollutants. The affordability and size of low-cost particle sensors makes them an attractive
 16 option for use in experiments requiring a number of instruments such as high density spatial
 17 mapping. However, for these low-cost sensors to be useful for these types of studies their
 18 accuracy and precision needs to be quantified. We evaluated the Alphasense OPC-N2, a
 19 promising low-cost miniature optical particle counter, for monitoring ambient airborne
 20 particles at typical urban background sites in the UK. The precision of the OPC-N2 was
 21 assessed by co-locating 14 instruments at a site to investigate the variation in measured
 22 concentrations. Comparison to two different reference optical particle counters as well as a
 23 TEOM-FDMS enabled the accuracy of the OPC-N2 to be evaluated. Comparison of the OPC-
 24 N2 to the reference optical instruments demonstrated reasonable agreement for the measured
 25 mass concentrations of PM₁, PM_{2.5} and PM₁₀. However, the OPC-N2 demonstrated a
 26 significant positive artefact in measured particle mass during times of high ambient RH
 27 (>85%) and a calibration factor was developed based upon κ -Kohler theory, using average
 28 bulk particle aerosol hygroscopicity. Application of this RH correction factor resulted in the
 29 OPC-N2 measurements being within 33% of the TEOM-FDMS, comparable to the agreement
 30 between a reference optical particle counter and the TEOM-FDMS (20%). Reasonable inter-
 31 unit precision for the 14 OPC-N2 sensors was observed. Overall, the OPC-N2 was found to



1 accurately measure ambient airborne particle mass concentration provided they are i)
2 correctly calibrated and ii) corrected for ambient RH. The reasonable level of precision
3 demonstrated between multiple OPC-N2 suggests that they would be suitable device for
4 applications where the spatial variability in particle concentration was to be determined.

5

6 **1.0 Introduction**

7 Airborne particles are of global concern due to their detrimental health effects, particularly in
8 the fine fraction (PM_{2.5}, particles with an aerodynamic diameter less than 2.5 µm) and as a
9 result are a regulated pollutant in the EU, USA and other states. Monitoring ambient particle
10 mass concentrations is typically performed using a small number of fixed instruments with
11 gaps in the spatial coverage usually estimated via modeling or interpolation. This is often
12 unsatisfactory as there can be micro-environments in urban areas that result in large spatial
13 and temporal inhomogeneity in airborne particle concentrations, which in turn makes
14 assessment of human exposure to airborne particles difficult (de Nazelle et al., 2017).

15 Into this gap a fast growing area is the development of low-cost sensors for measuring the
16 concentrations of a wide range of species in the atmosphere including gases and particles
17 (Lewis et al., 2016; Rai et al., 2017; Snyder et al., 2013). However the question remains as to
18 whether the uncertain quality of data from these low cost sensors can be of value when
19 attempting to determine pollutant concentrations at high spatial resolution (Kumar et al.,
20 2015). Sensors for both gases and particles can suffer from drift and a number of interference
21 artefacts such as relative humidity (RH), temperature and other gas phase species (Lewis et
22 al., 2016; Mueller et al., 2017; Popoola et al., 2016). Despite these challenges, recent work
23 has shown that low-cost gas sensors can be deployed in large scale networks provided
24 appropriate corrections for known artefacts are applied (Borrego et al., 2016; Mead et al.,
25 2013; Mueller et al., 2017), with clustering of multiple gas sensors into one unit shown to be
26 an effective methodology (Lewis et al., 2016; Mueller et al., 2017; Smith et al., 2017).

27 For low-cost particle sensors, their reported performance across the literature is somewhat
28 mixed (Borrego et al., 2016; Castellini et al., 2014; Sousan et al., 2016; Viana et al., 2015)
29 and can depend on the type of particle sensor employed. There are a wide range of low-cost
30 particle sensors available commercially by companies including from manufacturers
31 Dylos, TSI, Airsense and Alphasense. The more widely used and available low-cost particle



1 sensors can be considered as miniaturized versions of optical particle counters (OPC) and
2 employ a light scattering technique to measure ambient particle concentrations (See e.g. (Gao
3 et al., 2015; Sousan et al., 2016). While these miniature OPC are not meant to compete with
4 more established instrumentation in terms of their accuracy and precision, their affordability
5 and size makes them attractive for use in experiments requiring a number of such
6 instruments, such as personal monitoring (See e.g. (de Nazelle et al., 2017; Steinle et al.,
7 2015)). However to be useful in these types of studies, the precision and accuracy of these
8 instruments needs to be evaluated.

9 Laboratory assessments of the performance of a number of low-cost miniature OPC's have
10 shown promising results, with reasonable precision observed compared to reference
11 instrumentation (Manikonda et al., 2016). Sousan et al., (2016) evaluated the Alphasense
12 OPC-N2 in a laboratory study using reference aerosols (Arizona road dust, NaCl and welding
13 fumes) and found reasonable agreement for size distributions and particle mass between the
14 OPC-N2 and a GRIMM Portable Aerosol Spectrophotometer, provided appropriate and
15 specific calibrations were applied. While these results are encouraging (Manikonda et al.,
16 2016; Sousan et al., 2016), laboratory-based studies using reference aerosols may not be
17 representative of their performance when measuring ambient particles, owing in part to the
18 complex mixture and variable relative humidity and temperature encountered in the real-
19 world. Previous field testing of low-cost particle sensors has found that that Dylos (Steinle et
20 al., 2015), PUWP (Gao et al., 2015) performed well for ambient sampling of particle mass
21 concentration in both an urban and rural environments when compared to reference
22 instruments however were assessed over a short period (4-5 days). In contrast, at a roadside
23 location poor agreement between two different OPC sensors compared to reference
24 instruments was observed by Borrego et al. (2016). Clearly, the results are mixed and longer-
25 term assessment of the stability and longevity of these instruments are needed, as these are
26 critical parameters when considering their worth for use in large-scale networks.

27 We evaluate here the Alphasense OPC-N2, a promising low-cost miniature optical particle
28 counter (Sousan et al., 2016), for monitoring ambient airborne particles at typical urban
29 background sites in the UK. We assessed the inter-unit precision of the OPC-N2 by co-
30 locating 14 instruments at a single site to investigate the variation in measured particle mass
31 concentration in the PM_{10} , $PM_{2.5}$ and PM_1 size fractions between OPC-N2. In order to
32 determine the accuracy of the OPC-N2, we compared it to two well-established commercial



1 optical particle counters that employ a similar light scattering technique as well as a TEOM-
2 FDMS, a regulatory standard instrument for particle mass concentration measurements.

3 **2.0 Method**

4 **2.1 Instrumentation**

5 **2.1.1 Alphasense Optical particle sensor (OPC-N2)**

6 The Optical Particle Sensor (OPC) under evaluation in the current work is the OPC-N2
7 manufactured commercially by Alphasense (www.alphasense.com). The OPC-N2 can be
8 considered as a miniaturized OPC as it measures 75x60x65 mm and weighs under 105 g, and
9 as such is significantly cheaper (approx. £200) than the comparable reference instruments
10 (see next section). The OPC-N2 has a reported size range of 0.38 to 17 μm across 16 size
11 bins, and maximum particle count of 10,000 per second. All OPC-N2 in this study were
12 firmware version 18.

13 The OPC-N2 is designed to log data via a laptop using software supplied by Alphasense,
14 however this may not be practical when using multiple OPC-N2 at once or for personal
15 monitoring. Therefore, we developed a custom built systems for logging the OPC-N2 during
16 the inter-comparison, using custom-built logger utilizing Raspberry Pi 3 and Arduino
17 systems. The Python code to log the outputs from OPC-N2 on a Raspberry Pi 3 is made
18 available in the Supplementary Material. The Python code makes use of the py-opc python
19 library for operating the OPC-N2 written by Hagan (2017).

20 **2.1.2 Reference Instruments**

21 The first reference instrument was a TSI 3330 optical particle spectrophotometer (OPS),
22 which measures particles number concentrations between 0.3 – 10 μm across 16 size bins,
23 with a maximum particle count of 3000 particles cm^{-3} . A GRIMM Portable Aerosol
24 Spectrometer (PAS-1.108, forthwith referred to as the GRIMM) was also utilized, which
25 records particle number concentrations in 15 bins from 0.3 – 20 μm . The TSI 3330 and
26 GRIMM were both recently calibrated and serviced. All measurements of airborne particle
27 concentrations are inherently operationally defined and as a result the TSI 3330 and the
28 GRIMM were chosen as reference instruments as they measure particle size in similar size
29 bins by a similar photometric technique to the Alphasense OPC-N2.



1 For the sake of this inter-comparison, we have taken the TSI 3330 and GRIMM data as an
2 accurate measure of particle mass concentrations. The reference instrument used for the
3 factory calibration of the OPC-N2 by Alphasense is the TSI 3330 (Sousan et al., 2016) and
4 hence included for comparison.

5 **2.2 Inter-comparison locations**

6 **2.2.1 Elms Rd Observatory Station**

7 The instruments were housed within the Elms Road Observatory Station (EROS) located on
8 the University of Birmingham campus. The site is classed as urban background, with
9 emissions from nearby road and a construction site the major sources of particles. Fourteen
10 OPC-N2 were deployed at EROS, enabling the precision of the OPC-N2 to be assessed along
11 with the accuracy relative to the reference instruments, the TSI 3330 and GRIMM. An
12 intensive inter-comparison ran for just over 5 weeks, from 26th August till 3rd October 2016,
13 during which all 14 OPC-N2, TSI 3330 and GRIMM sampled ambient air. Minimal lengths
14 of stainless steel tubing (OPC-N2) and conductive black tubing (TSI 3330 and GRIMM)
15 were used to sample outside air, with each OPC having its own inlet at a height of 1.5 m.
16 Sampling intervals for the OPC-N2, TSI 3330 and GRIMM were 10, 60 and 6 seconds,
17 respectively. In addition, measurements from the nearby Elms Road Meteorological station
18 were also obtained which is located approximately 100 m away from EROS.

19 At the conclusion of the intensive inter-comparison, a subset of the OPC-N2 (5) continued to
20 sample at EROS along with the GRIMM, to test the robustness and suitability of the OPC-N2
21 for longer-term monitoring. The long-term monitoring concluded on 1 February 2017,
22 meaning that these OPC-N2 sampled ambient air for up to 5 months.

23 **2.2.2 Tyburn Rd**

24 For regulatory purposes, an accepted method for measuring particle mass concentrations is a
25 Tapered Element Oscillating Microbalance (TEOM) and therefore we also compared the
26 OPC-N2 to this technique despite the difference in particle measurement approaches. An
27 urban background air monitoring station part of the UK Automatic and Rural Urban Network
28 (AURN) nearby EROS (Tyburn Rd) was chosen for this inter-comparison. At the Tyburn Rd
29 AURN station, the TEOM monitor was fitted with a Filter Dynamic Measurement System
30 (FDMS) (Grover et al., 2006). A subset of OPC-N2 (4) and the GRIMM PAS 1.108 that were



1 deployed at EROS sampled at Tyburn Rd station for 2 weeks during February 2017. The
 2 OPC-N2 was housed individually within waterproof boxes on the roof of the cabin near to the
 3 TEOM inlet in order to keep the inlet length the same as used at EROS. The GRIMM
 4 sampled from a nearby separate inlet.

5 2.3 Data Analysis

6 All OPC employed in this study count the number of particles and determine the size based
 7 upon particle light scattering of a laser, and to convert to particle mass concentration must
 8 apply a number of assumptions. To calculate the particle mass concentration, spherical
 9 particles of a uniform density and shape are assumed, which is not strictly true for airborne
 10 particles in an urban atmosphere but is considered a reasonable approximation. Therefore to
 11 ensure a fair comparison between the different OPC, the same calculations and assumptions
 12 must be applied to all three OPC measurements. The TSI 3330 data was processed using the
 13 TSI AIM software to convert the particle count concentration to particle mass measurements.
 14 The particle counts from the GRIMM data was converted to particle mass (via particle
 15 volume) using the same calculations, as outlined in the TSI AIM software manual according
 16 to Equations 1 to 3:

$$17 \quad D_{pv} = LB \left[\frac{1}{4} \left(1 + \left(\frac{UB}{LB} \right)^2 \right) \left(1 + \left(\frac{UB}{LB} \right) \right) \right]^{\frac{1}{3}} \quad (1)$$

$$18 \quad v = \frac{\pi D_{pv}^3 n}{6} \quad (2)$$

$$19 \quad m = \rho v \quad (3)$$

20 where D_{pv} is the volume weighted diameter, LB the channel lower boundary, UB the channel
 21 upper boundary, v is the particle volume for a channel, n is number weighted concentration
 22 per channel, m is the particle mass per channel and ρ is the particle density.

23 The OPC-N2 converts, on board via a factory determined calibration, particle counts to
 24 particle mass concentration in PM_{10} , $PM_{2.5}$ and PM_{10} mass concentrations. There is no further
 25 information provided by Alphasense on how this calculation is performed apart from the
 26 applied particle density across all size bins was 1.65 g cm^{-3} . Therefore, we assumed



1 calculations are similar to Eqns 1 and 2 as applied to the TSI and GRIMM data and used the
2 same particle density (1.65) across all size bins to calculate particle mass for all OPC.

3 All instrument time series were corrected for drift against a reference time. As the sampling
4 intervals varied slightly between the different OPC, a 5 min average of particle
5 concentrations was used for inter-comparison between instruments.

6 **3.0 Results and Discussion**

7 **3.1 EROS inter-comparison**

8 **3.1.1 Comparison of reference optical light scattering instruments**

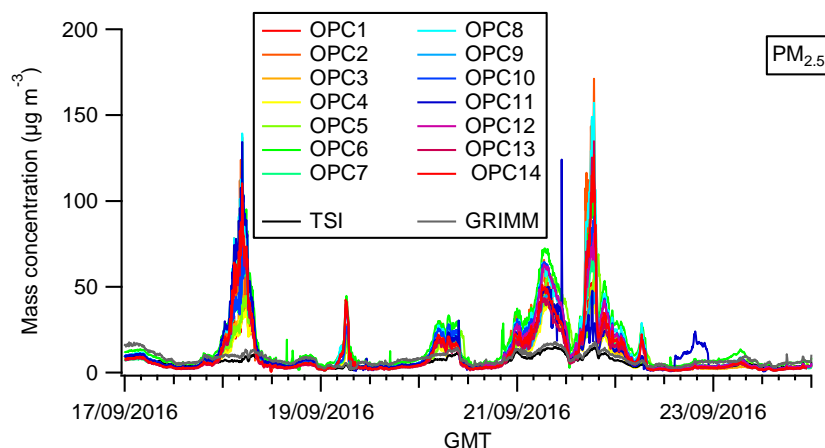
9 The two light scattering optical particle counters used as reference instruments in this study
10 were found to be well correlated ($r^2 > 0.9$), with the GRIMM recording between 20-30%
11 higher concentrations for all three particle mass fractions (Fig S1, Supporting Information).
12 The GRIMM is known to overestimate number concentration (Sousan et al., 2016 and
13 references therein) and this difference may reflect differing efficiencies in particle detection
14 between the two instruments.

15 **3.1.2 Performance of the OPC-N2**

16 The performance of the custom built logging systems varied between 44-94% successful data
17 capture, with the Arduino and Raspberry Pi systems giving 44-65% and >92%, respectively.
18 The Raspberry Pi data logger system was used for the long-term measurements and for the
19 inter-comparison with the AURN site due to its better performance. The data losses were due
20 to hardware issues and not related to performance of the OPC-N2. Due to the missing data,
21 only a subset of measured $PM_{2.5}$ concentrations when all 14 OPC-N2 were logging are shown
22 in Fig 1, along with measured concentrations by the reference instruments. From Fig 1, while
23 there are times when there appears to be excellent agreement between the OPC-N2 and the
24 reference instruments, there are times when the OPC-N2 record a significant positive artefact,
25 and during these times the spread in measured concentrations increases. For example, on the
26 morning of the 18th September, the range of measured concentrations by the individual OPC-
27 N2 was from approximately $30\text{--}150\ \mu\text{g m}^{-3}$, whereas the reference instruments reported ~ 10
28 $\mu\text{g m}^{-3}$. The cause of the positive artefact is investigated in later sections, but it points to the
29 individual OPC-N2 responding differently to this artefact. Similar trends were also observed
30 for PM_1 and PM_{10} , see Figure S2 in the Supporting Information.



1



2

3 Figure 1: Time series of $PM_{2.5}$ concentrations measured by all OPC-N2 and the reference
 4 instruments, TSI 3330 and GRIMM for selected period with high OPC-N2 data coverage.

5 As there is a considerable spread in response for the OPC-N2 relative to the reference
 6 instruments, we then quantified whether it was always the same OPC-N2 reading low and
 7 high. Due to the aforementioned data capture issues, this analysis was only applied to days
 8 when all 14 OPC-N2 were running, 21st-24th September (Fig 1). The results are shown as a
 9 rank order plot, where the OPC-N2 observations are ordered from the highest reported value
 10 to the lowest over this period, normalised to the median concentration at the start of the
 11 analysis ($t=0$), shown for $PM_{2.5}$ mass concentration in Figure 2. The ranking of the OPC-N2's
 12 showed some variability over time within periods of 1-6 hours, which was particularly
 13 noticeable during periods when the OPC-N2 signals underwent large changes in
 14 concentrations. This demonstrates that the highest reporting OPC was not consistently
 15 reporting the highest and lowest the lowest $PM_{2.5}$ concentration over the whole 3 day period.
 16 The same trend was also observed for PM_{10} and PM_{10} mass concentrations, as shown in Figure
 17 S3 (Supporting Information).

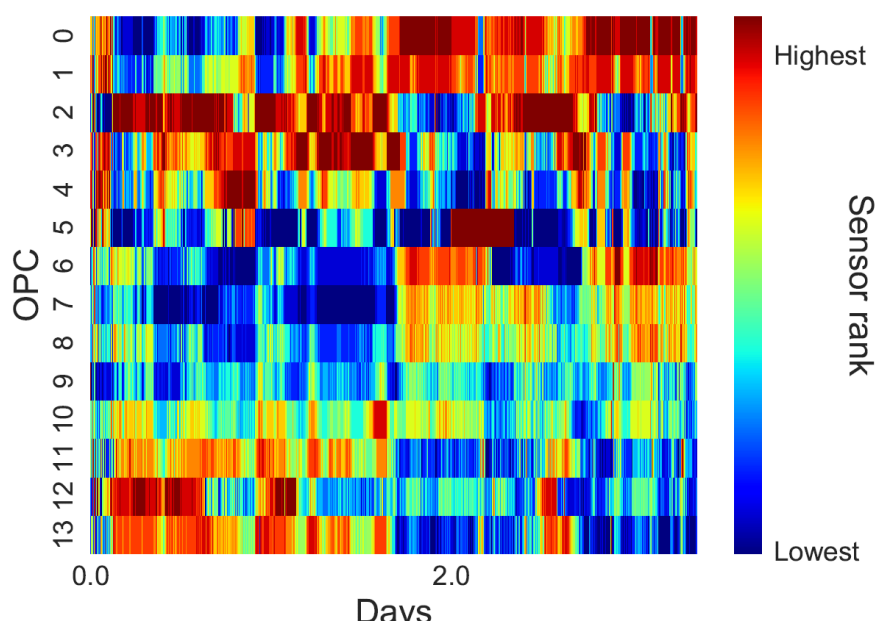
18

19 For the 3 day time period (21st-24th of September) we applied the rank order analysis, two
 20 subsets of concentrations measured by the OPC-N2 were evident in the time series (Fig 1);
 21 one a period of highly variable mass concentrations (0:00 21/9/16 to 12:00 22/9/16) of
 22 September) followed by more stable mass concentrations (12:00 22/9/16 onward). This was
 23 reflected in the corresponding rank order plots where relatively consistent OPC rank orders
 24 were observed throughout the variable and comparatively stable PM concentrations periods.



1 However, there is a noticeable transition between the two periods in the rank order plot,
 2 observed at approximately 12:00 on the 22nd). This transition in rank orders would reflect the
 3 difference in OPC PM sensitivities, random noise and offset values between each OPC. Over
 4 the 3 day period the OPCs appeared to hold their response characteristics and hence rank
 5 orders well, suggesting that over this timescale quantitative concentrations could be directly
 6 compared. Due to the changing response and the incomplete data coverage, for the rest of the
 7 analysis in this paper, when comparing to the reference instruments the median and inter-
 8 quartiles concentrations of all 14 OPC-N2 were used.

9



10

11

12 Figure 2: Sensor ranking analysis for measured $PM_{2.5}$ mass concentrations for the 14 OPC-
 13 N2 over a 3 day period (21st-24th of September) with high OPC-N2 data coverage.

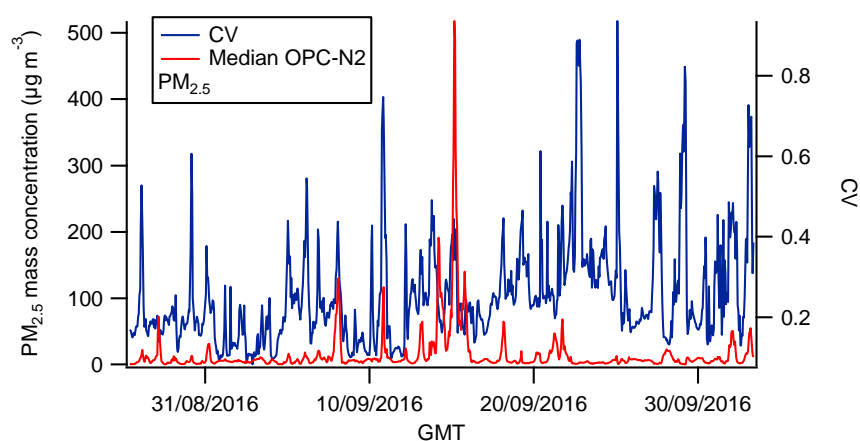
14

15 One measure of the precision of a group of instruments is the coefficient of variance (CV)
 16 and this was calculated for the measured ambient mass concentrations of all 14 OPC-N2 to
 17 assess the variability between 14 instruments. The average CV was 0.32 ± 0.16 , 0.25 ± 0.14 and
 18 0.22 ± 0.13 for PM_1 , $PM_{2.5}$ and PM_{10} mass concentrations, respectively. This is higher than the
 19 value of 0.1 considered acceptable for duplicate instruments by the US EPA (see Sousan et
 20 al., 2016 and references therein) but perhaps not unreasonable for low-cost sensors. This may



1 in part be due the OPC-N2 all sampling from separate but identical inlets but suggests the
2 precision of the OPC-N2 would need to be considered when comparing multiple units. To
3 analyse whether the CV for the OPC-N2 varied over the month, the median concentration
4 was plotted along with the CV (shown for $PM_{2.5}$ in Fig 3). Throughout the measurement
5 period, the CV was fairly consistent, with spikes in CV values evident during periods of high
6 $PM_{2.5}$ concentrations, in agreement with trends observed in Fig 1. We observed a similar
7 trend of consistent CV values for both PM_{10} and PM_{10} concentrations suggesting reasonably
8 stable agreement between all OPC-N2 over a 5 week period.

9



10

11 Figure 3: Time series of the hourly average median OPC and CV during the September
12 intensive inter-comparison at EROS for $PM_{2.5}$ mass concentration.

13 3.2 Comparison of Alpha sense OPC to reference instruments

14 3.2.1 Particle mass concentration measurement at EROS

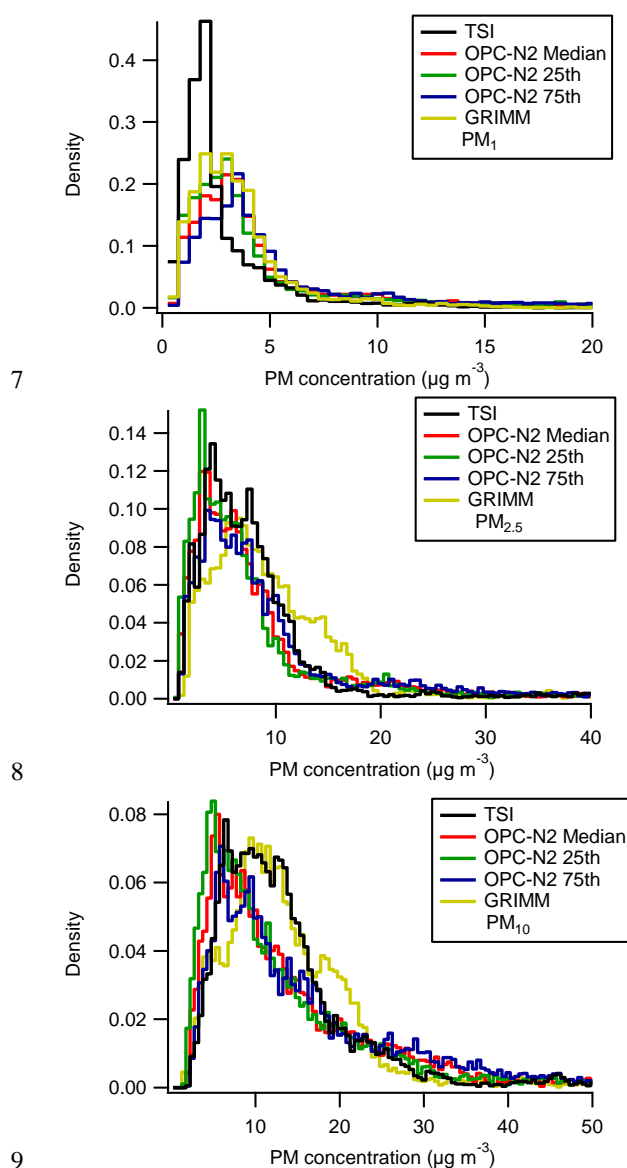
15

16 The median and inter-quartiles of the measured PM concentrations from the 14 OPC-N2 were
17 used to compare the measured particle mass concentrations to the reference instruments
18 (Figure 4). From Fig 4, the notably similar distributions across all three particle size fractions
19 for the first and third quartiles indicate good agreement between the 14 OPC-N2, further
20 highlighting the reasonable degree of precision between the OPC-N2 as shown in the
21 previous section. At typical ambient $PM_{2.5}$ and PM_{10} mass concentrations for the UK, similar
22 distributions were observed for the OPC-N2 and reference instruments (Fig 1), suggesting
23 reasonable agreement between the devices. In contrast, different distributions were observed



1 for the PM_{10} fraction, with the OPC-N2 and GRIMM in agreement but appearing to over-
 2 estimating the PM_{10} mass concentrations with respect to the TSI 3330. While the OPC-N2 has
 3 a higher particle size cut-off ($0.38 \mu m$) compared to the TSI ($0.3 \mu m$) and may explain the
 4 observed difference in frequency distribution for PM_{10} (Fig 1), the TSI and GRIMM have the
 5 same particle size cut-off ($0.3 \mu m$) and so would be expected to agree.

6





1 Figure 4: Histogram of measured PM_{10} , $PM_{2.5}$ and PM_{10} mass concentrations by the TSI 3330,
 2 GRIMM and median and inter-quartile values for the 14 OPC-N2. Note the different x and y
 3 axis scales.

4 When the median and inter-quartile OPC-N2 concentrations were plotted against the TSI and
 5 GRIMM concentrations, the slope was greater than unity for all three size fractions (Table 1)
 6 indicating that the OPC-N2 were over-estimating the ambient particle mass concentrations
 7 (approx. 2 to 5 times, Table 1). Overall, the OPC-N2 and GRIMM were in better agreement
 8 compared to the TSI for all size fractions (Table 1). The GRIMM was found to record PM
 9 concentrations 20-30% higher compared to the TSI (Figure S1), and this could in part
 10 account for the observed lower slopes between the GRIMM and the OPC-N2.

11 Table 1: Slopes of measured PM mass concentrations of the reference instruments against the
 12 median and inter-quartiles for OPC-N2. Correlation co-efficient, r^2 is given in parenthesis.

	PM_{10}		$PM_{2.5}$		PM_{10}	
<i>OPC-N2</i>	<i>TSI</i>	<i>GRIMM</i>	<i>TSI</i>	<i>GRIMM</i>	<i>TSI</i>	<i>GRIMM</i>
25th	2.93+0.01 (0.9)	2.34+0.1 (0.92)	3.16+0.03 (0.66)	2.62+0.02 (0.77)	2.05+0.02 (0.64)	1.85+0.02 (0.6)
Median	3.19+0.02 (0.86)	2.63+0.01 (0.91)	3.53+0.04 (0.63)	3.02+0.03 (0.76)	2.29+0.03 (0.57)	2.06+0.02 (0.67)
75th	3.90+0.02 (0.87)	3.24+0.02 (0.89)	4.77+0.06 (0.59)	4.21+0.04 (0.71)	2.73+0.04 (0.53)	2.47+0.35 (0.57)

13
 14 The time series of the median OPC-N2 $PM_{2.5}$ concentrations along with the two reference
 15 instruments are shown in Figure 5, and for a large portion of the inter-comparison all
 16 instruments appear to be in reasonable agreement. However, there were a number of times
 17 when the OPC-N2 readings were up to an order of magnitude higher relative to the reference
 18 (e.g. 15th September), pointing to a significant instrument artefact. On the 15th September, the
 19 GRIMM and TSI also move out of agreement and may point to the same artefact affecting the
 20 GRIMM. Similar trends were also observed for the PM_{10} and PM_{10} mass fractions (Fig S4,
 21 Supporting Information) with the OPC-N2 over-estimating the PM_{10} concentration by several
 22 orders of magnitude on 15th September (peak mass concentrations in the order of 15,000 μg
 23 m^{-3}). Note that as EROS is an urban background site, it was unlikely to be affected by plumes



1 from sources such as vehicles and as a result these high concentrations spikes may not be
2 real.

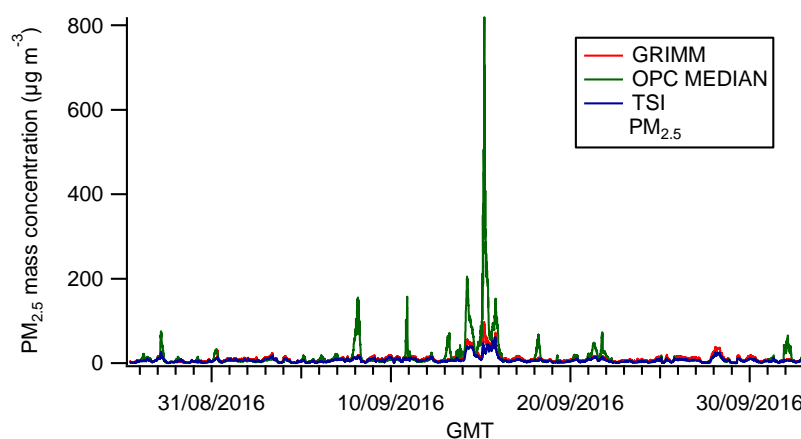
3

4 The factors contributing to this apparent artefact shown by the OPC-N2 were investigated. In
5 Fig 6, the agreement between the OPC-N2 and the TSI instrument appears to vary as a
6 function of ambient RH, with reasonable agreement observed between the two instruments
7 during periods of relatively low ambient RH. However, during times when the RH was high
8 (>90%), the OPC-N2 recorded concentrations markedly higher than that measured by the TSI
9 3330 (Fig 6). Thus, it points to ambient RH as a significant contributing factor affecting the
10 particle mass concentrations measured by the OPC-N2, and this is tested further in later
11 sections. There are distinct differences in design in OPC-N2 compared to the reference
12 instruments (GRIMM and TSI 3330) as both the TSI 3330 and GRIMM utilise a sheath flow
13 unlike the OPC-N2. The sheath flow in both devices will be warmed to temperatures higher
14 than the ambient air due to proximity to the instrument pumps and electronics. This would
15 mean that they measure at a lower RH than ambient and could explain why no RH
16 dependence was observed on measured particle concentrations by the GRIMM and TSI 3330.

17

18

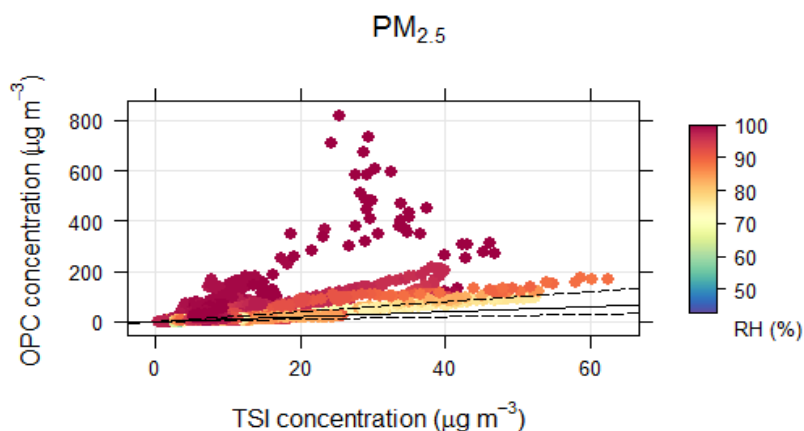
19



20

21 Figure 5: Time series of the measured $PM_{2.5}$ mass concentrations by the TSI, GRIMM and
22 median concentration measured by the14 OPC-N2 at EROS.

23



1
 2 Figure 6: Measured concentrations by the TSI 3330 compared to the median concentration
 3 measured by the 14 OPC-N2, coloured by the ambient relative humidity. Also shown are the
 4 1:1 (solid) and 0.5:1 and 2:1 (dashed) lines.

6 3.2.3 Comparison to TEOM-FDMS at AURN monitoring station

7
 8 We deployed a subset of the OPC-N2 devices (4) and the GRIMM at an urban background
 9 AURN station, to enable comparison of the measured ambient particle mass concentrations to
 10 a TEOM-FDMS. The time series of the measured concentrations of PM_{10} and $PM_{2.5}$ for all
 11 instruments is shown in Fig 7. The two reference instruments were found to be well
 12 correlated ($r^2 > 0.91$, Figure S7, Supporting Information) but with the GRIMM reading was
 13 about 20% lower than the TEOM, in agreement with previous work (Grover et al., 2006).
 14 From Fig 6, periods of agreement between the four OPC-N2 and the reference instruments
 15 (GRIMM and TEOM) were apparent, along with times when the four OPC-N2 measured
 16 concentrations that were notably higher than the reference instruments. Overall, when
 17 compared to the TEOM, the OPC-N2 measurements were 2.5-3.9 times higher for both the
 18 PM_{10} and $PM_{2.5}$, with considerable scatter observed (Table 2).

19

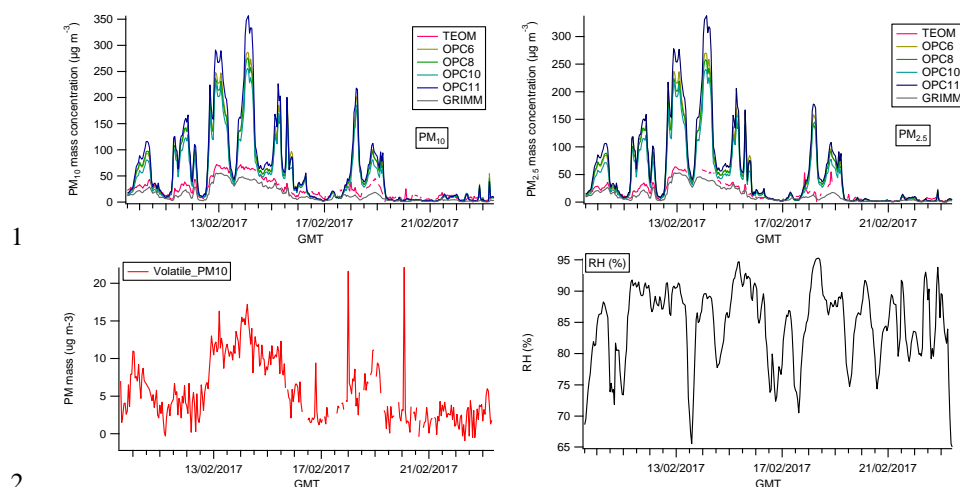


Figure 7: Time series for hourly measured PM mass concentrations by the TEOM, four OPC-N2 and GRIMM at Tyburn Rd urban background AURN station. Relative humidity measured at Tyburn Rd also shown.

Closer inspection of Fig 7 indicated that the times when the four OPC-N2 over-estimated the particle mass concentrations were during times of high RH (e.g. 12-14th Feb), as observed in the previous section. However, there were periods of high RH when the four OPC-N2 and TEOM were in better agreement (e.g. 20th Feb onwards), indicating that the large positive artefact observed in the OPC-N2 was not just related to RH. Rather, it appears that positive artefact was observed during times when the volatile fraction measured by the TEOM was relatively high, as well as higher RH, as was observed on 12-14th Feb (Fig 7). Thus, it suggests that the ambient aerosol composition also contributed to the significant positive artefact in the OPC-N2. A recent laboratory study found that the particle mass concentrations measured by OPC-N2 for all three size fractions were highly linear with respect to gravimetrically corrected reference instruments but that the slope was dependent on the aerosol type (Sousan et al., 2016). Sousan et al. (2016) observed in the PM₁₀ fraction slopes greater than unity for Arizona road dust but less than unity for salt and therefore suggest that changes in aerosol composition may also account for the differences observed between the reference instruments and OPC-N2 (Figs 7). This result highlights a limitation when comparing optical methods to gravimetric - as differences may be due to changes in particle mass, size distribution or composition: as all can affect the ability of a particle to scatter light (Holstius et al., 2014).



1
 2 From Fig 6, the times when there was a large positive artefact in the OPC-N2 occurred when
 3 the RH was above 85%. If we exclude these times when the RH was over this threshold,
 4 better agreement between the four OPC-N2 and the TEOM was observed, with slopes
 5 between 1.1-1.7 for both size fractions (Table 2). One of the OPC-N2 recorded notably
 6 higher mass concentrations compared to the reference instruments (OPC11), compared to the
 7 other three OPC-N2 (Table 2), and this highlights the need to calibrate each OPC individually
 8 before use in field measurements.

9
 10 Table 2: Slopes of measured PM mass concentrations of the reference instruments (TEOM
 11 and GRIMM) against the OPC-N2. The correlation co-efficient, r^2 is given in parenthesis.

		PM ₁₀				PM _{2.5}			
		OPC6	OPC8	OPC10	OPC11	OPC6	OPC8	OPC10	OPC11
ALL	TEOM	2.6	2.8	2.5	3.5	3.3	3.1	2.9	3.9
		(0.64)	(0.68)	(0.64)	(0.67)	(0.7)	(0.74)	(0.7)	(0.72)
	GRIMM	3.7	3.6	3.2	4.4	3.8	3.7	3.4	4.6
		(0.66)	(0.69)	(0.66)	(0.68)	(0.71)	(0.74)	(0.71)	(0.72)
<85% RH	TEOM	1.4	1.4	1.2	1.7	1.3	1.4	1.1	1.6
		(0.82)	(0.83)	(0.83)	(0.83)	(0.79)	(0.8)	(0.79)	(0.79)
	GRIMM	1.8	1.9	1.6	2.2	2.0	2.1	1.7	2.4
		(0.83)	(0.84)	(0.84)	(0.84)	(0.89)	(0.89)	(0.9)	(0.88)

13 14 3.3 Development of correction factor for ambient RH

15 Clearly there were times when there was a significant instrument artefact for the OPC-N2
 16 (Figs 4 and S4) and the highest over-estimations occurred at high RH at both EROS and
 17 Tyburn Rd (e.g. Fig 5 and 6). The size of hygroscopic particles is known to be dependent on
 18 RH, as the particle refractive index and size are both a function of RH. Inorganic aerosols
 19 (e.g. sodium chloride, nitrate and sulphate), make up a large portion of the PM₁₀ observed at
 20 EROS (Yin et al., 2010), and are known to demonstrate an exponential increase in
 21 hygroscopic growth at high RH (e.g. (Hu et al., 2010; Pope et al., 2010)).



1 The ratio of measured mass concentrations by the OPC-N2 relative to the reference
2 instruments was plotted as a function of RH, and appeared to show an exponential increase
3 above ~85% RH, similar to hygroscopic particle growth curves (Pöschl, 2005). As a result,
4 we applied κ -Kohler theory (Petters and Kreidenweis, 2007), which describes the relationship
5 between particle hygroscopicity and volume by a single hygroscopicity parameter, κ . The κ -
6 Kohler theory can be adapted to relate particle mass to hygroscopicity at a given RH by
7 equation 5 (Pope, 2010):

$$9 \quad a_w = \frac{(m/m_o - 1)}{(m/m_o - 1) + (\frac{\rho_w}{\rho_p} \kappa)} \quad (5)$$

10

11 Where a_w is the water activity ($a_w = \text{ambient RH}/100$), m and m_o are the wet and dry (RH =
12 0%) aerosol mass, respectively. The density of the dry particles and water is given by ρ_w and
13 ρ_p , respectively. The density of water is 1 g cm^{-3} , and the bulk dry particle density is assumed
14 to be 1.65 g cm^{-3} . The value for κ can be found by a non-linear curve fitting of a humidogram
15 (m/m_o vs a_w), and was calculated using the TEOM measurements at Tyburn Rd in the first
16 instance as the TEOM system employs a Nafion dryer and so measures dry particle mass
17 (Grover et al., 2006). To account for the differences in mass concentration measured by the
18 TEOM and OPC-N2 at RH less than 85%, the scaling factors shown in Table 2 are used
19 to calibrate the dry mass of the OPC-N2 to that observed in the TEOM, both in the $\text{PM}_{2.5}$ and
20 PM_{10} fractions.

21

22 Figure 8 shows the humidogram plots, for both the $\text{PM}_{2.5}$ and PM_{10} fractions, obtained by
23 plotting the ratio of OPC-N2 to the reference instrument (TEOM and GRIMM) outputs
24 versus RH. When using the TEOM for m_o , similar κ constants were calculated for all OPC-
25 N2, ranging from 0.38-0.41 and 0.48-0.51 for $\text{PM}_{2.5}$ and PM_{10} , respectively, which is within
26 the expected range for Europe (0.36 ± 0.16 , (Pringle et al., 2010). Similar κ values were
27 observed when using the GRIMM mass concentrations as the dry particle mass (m_o), ranging
28 from 0.41-0.44 and 0.38-0.41 for $\text{PM}_{2.5}$ and PM_{10} , respectively.

29

30

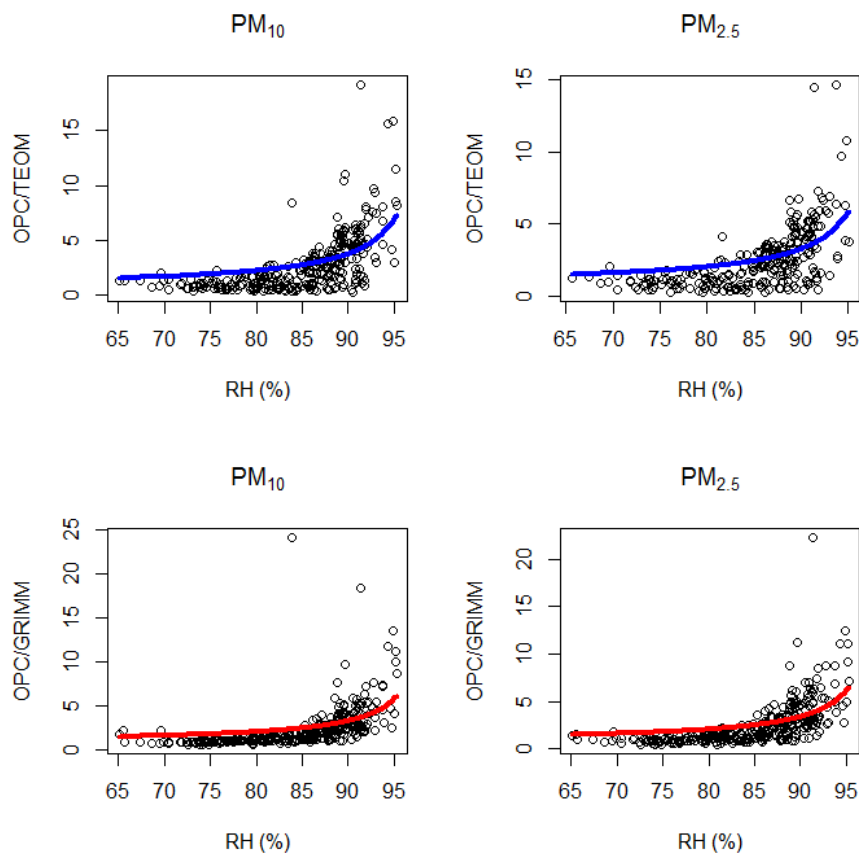


Figure 8: Measured and fitted humidograms (m/m_0 vs RH) recorded at the Tyburn Road AURN site for PM_{10} and $PM_{2.5}$ size fractions and reference instruments (TEOM and GRIMM). The dry mass (m_0) is given by the TEOM or GRIMM and the humidified mass is given by the OPC-N2. Measured data is given by the black circles, the fitted data is given by the blue (TEOM-FDMS) and red (GRIMM) line.

We then applied this fitting constant to model the expected OPC/Reference instrument ratio for a given RH as a result of particle hygroscopic growth, by re-arranging Equation 5:

$$\frac{m}{m_0} = 1 + \frac{\frac{\rho_w \kappa}{\rho_p}}{-1 + \frac{1}{a_w}} \quad (6)$$



1 Where the m/m_0 is the ratio of the OPC-N2 to the reference instruments. Using Equation 6,
 2 the mass concentrations measured by the OPC-N2 were corrected and significantly better
 3 agreement between the corrected OPC-N2 and reference instruments was observed for
 4 measurements across the whole range of ambient RH (Tables 2 and 3). Overall, the corrected
 5 OPC-N2 mass concentrations using Eqn 6 were notably better, within 33% and 52% of the
 6 TEOM and GRIMM, respectively. (Table 3) compared to 250-400% without the correction
 7 factor (Table 2). The time series for the corrected data is shown in Figures S8 and S9
 8 (Supporting Information) and there are periods where there is good agreement between TEOM
 9 and the corrected OPC-N2.

10 There were also times when the OPC-N2 were clearly over-corrected (e.g. from 20th February
 11 onwards), generally when the ambient RH was low (Fig 6). This suggests that when the RH
 12 was below a threshold, Eqn 6 overcorrects the data and this can be observed in the
 13 humidograms shown in Figure 8. Typically, at RH <80% the hygroscopic growth of real
 14 atmospheric aerosols is small and it may be more appropriate to apply a linear regression
 15 correction factor for data recorded under these RH conditions. During the period from the
 16 20th February, the volatile particle fraction was also lower (Fig 6) and this indicates a
 17 significantly different aerosol composition. Since κ is composition dependent, a single global
 18 fit to κ will result in poor fitting when the true κ is significantly different to the average κ .
 19 The preceding discussion suggests that further refinement to the correction factors applied to
 20 the OPC-N2 is possible, depending on the ambient RH and better knowledge of aerosol
 21 composition. RH measurement is relatively trivial and can be achieved with small sensors but
 22 aerosol composition determination still requires significant analytical equipment and
 23 expertise.

24

25 Table 3: Summary of the comparison between the corrected OPC-N2 (via Eqn 6) against the
 26 reference instruments

OPC-N2	TEOM		GRIMM	
	$PM_{2.5}$	PM_{10}	$PM_{2.5}$	PM_{10}
OPC6	1.08±0.03	0.87±0.02	1.26±0.03	1.27±0.03
OPC8	1.11±0.03	0.89±0.02	1.29±0.03	1.23±0.03
OPC10	0.98±0.03	0.80±0.02	1.16±0.03	1.17±0.03
OPC11	1.33±0.04	1.06±0.03	1.53±0.04	1.51±0.04

27



3.3.1 Longer-term monitoring with OPC-N2 at EROS

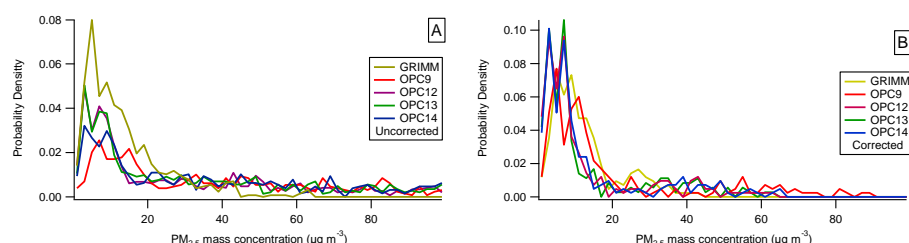


Figure 9: Histogram of measured $PM_{2.5}$ concentrations by the GRIMM PAS 1.108 and the 4 OPC-N2s for January. The uncorrected OPC-N2 concentrations are shown in the left plot (A), while the right plot (B) shows the RH corrected OPC-N2 concentrations.

After the conclusion of the intensive measurements at EROS (Section 3.1), five of the OPC-N2 continued monitoring for a further 4 months to examine if there was any evidence of instrument drift over time, along with the GRIMM as reference. One of the OPC-N2 failed in December, and so was excluded from this analysis. The remaining four OPC-N2 were compared to GRIMM and in January after running for 4 months (Fig 9A), and while two of the OPC-N2 had a similar distribution to the GRIMM (OPC13 and 14), the other two OPC-N2 appeared to show evidence for instrument drift as the mode has shifted relative to the GRIMM. However, the increased frequency of higher mass concentrations not observed by the GRIMM but by all four OPC-N2 (Fig 9A) suggests that ambient RH is also a factor, as the average RH in January (91%) was higher than September (84%). Therefore, we calculated the correction for RH as described in the previous section (Eqn 6), as changes in aerosol composition would affect the particle hygroscopicity. In addition, the κ was only fitted for the data with $RH < 95\%$ since the hygroscopicity of aerosol is highly sensitive to any error in the RH measurement above this value. Application of the RH correction factor resulted in better agreement between each of the OPC-N2, with similar corrected distributions observed (Fig 9B). Furthermore, the corrected OPC-N2 concentrations also had better agreement with the GRIMM during January (Fig 9B) compared to uncorrected concentrations (Fig 9A), suggesting that changes in the particle water content were the cause.



1 Thus, at least over a four month measurement period, there appears to be no evidence for
2 instrument drift in the OPC-N2, once appropriate correction factors were applied.

3 3.4 Discussion on the OPC-N2 interferences

4 In the previous sections, the significant positive artefact observed by the OPC-N2 relative to
5 the reference instruments were at times when the ambient RH was high, pointing to particle
6 water content as the cause. This result is perhaps not surprising, as many studies in the
7 literature have shown that particle water content can be a major reason for discrepancies
8 between techniques that measure ambient particle mass (See e.g. (Charron et al., 2004)). The
9 use of κ -Kohler theory to derive a correction factor based on ambient RH improved the
10 agreement between the OPC-N2 and reference instruments; however a limitation of this
11 approach is that the bulk aerosol hygroscopicity is related to particle composition, typically
12 the inorganic fraction (e.g. (Gysel et al., 2007)). Variation in ambient particle composition
13 could account for the large spread observed in the ratio of OPC-N2/TEOM at high RH (Fig
14 7), as an average hygroscopicity correction will overestimate when PM with higher
15 hygroscopicity is measured and vice versa. Furthermore, Eqn 6 may not be required for
16 locations where the ambient RH is lower than 85%, as typically atmospheric particle growth
17 due to water below this threshold is limited and a simple linear regression may be sufficient.
18 Thus, in-situ and seasonally specific calibrations for the OPC-N2 are required to account for
19 possible differences in ambient aerosol properties. However as κ values for continental
20 regions tend to fall within a narrow range globally (0.3 ± 0.1 , (Andreae and Rosenfeld, 2008),
21 with some systematic deviations for certain regions (Pringle et al., 2010), this average κ value
22 could be used in lieu of calibration with reference instrument (e.g. a TEOM) to determine the
23 correction factor (C) according to Eqn 7:

$$25 \quad C = 1 + \frac{0.3/1.65}{-1 + \frac{1}{a_w}} \quad (7)$$

26
27 However, it should be noted that while *in situ* calibration of an OPC-N2 with suitable
28 reference instrumentation is preferable, for many locations around the world, and especially
29 low and middle income countries (LMICs), this may not be possible and so using an
30 appropriate κ value from the literature in Eqn 7 may be a reasonable approximation.

31



1 **4.0 Applicability of OPC-N2 for ambient monitoring**

2 The Alphasense OPC-N2 was evaluated for use in ambient monitoring of airborne particle
3 mass concentration, with TEOM-FDMS and two commercial optical light scattering
4 instruments; GRIMM PAS 1.108 and TSI 3330 employed as reference instruments.
5 Comparison of the OPC-N2 to the reference optical instruments demonstrated reasonable
6 agreement for the measured mass concentrations of PM_{10} , $PM_{2.5}$ and PM_{10} . However, the
7 OPC-N2 demonstrated a significant large positive artefact in measured particle mass during
8 times of high ambient RH, and a calibration factor was developed based on bulk particle
9 aerosol hygroscopicity. Application of the RH correction factor, based upon κ -Kohler theory,
10 resulted in notable improvement with the corrected OPC-N2 measurements within 33% of a
11 TEOM-FDMS. While higher than the slope of 1 ± 0.1 allowed by US EPA, it is comparable to
12 the agreement of a GRIMM to the TEOM (20%). All low cost PM sensors will likely require
13 calibration factors to obtain the dry particle weight unless they actively dry the PM
14 containing air stream before it enters the device. The use of heated inlets could be used to
15 reduce the RH in the air stream but would have knock on consequences on the power
16 requirements of the sensor, potentially making them less attractive for battery led operation.
17 Reasonable precision between 14 OPC-N2 employed in the study was observed, with CV of
18 $22 \pm 13\%$ for PM_{10} mass concentrations, with some of the variability likely due to use of
19 separate but identical inlets.
20 Overall, while the OPC-N2 have been shown to accurately measure ambient airborne particle
21 mass concentration provided they are correctly calibrated and corrected for RH. The
22 reasonable level of precision demonstrated between multiple OPC-N2 suggests that they
23 would be suitable for applications where a number of instruments are required such as spatial
24 mapping and personal exposure studies.

26 **Acknowledgements**

27 The authors wish to thank Peter Porter and Birmingham City Council for help in collocating
28 the sensors next to the Tyburn Road AURN site. Funding is acknowledged from EPSRC
29 (Global Challenges Research Fund IS2016). AL and MS acknowledge funding from the
30 NERC National Capability programme ACREW and NE/N007115/1



1 References

- 2 Andreae, M.O., Rosenfeld, D., 2008. Aerosol–cloud–precipitation interactions. Part 1. The
3 nature and sources of cloud-active aerosols. *Earth-Science Reviews* 89, 13-41.
- 4 Borrego, C., Costa, A.M., Ginja, J., Amorim, M., Coutinho, M., Karatzas, K., Sioumis, T.,
5 Katsifarakis, N., Konstantinidis, K., De Vito, S., Esposito, E., Smith, P., André, N., Gérard,
6 P., Francis, L.A., Castell, N., Schneider, P., Viana, M., Minguillón, M.C., Reimringer, W.,
7 Otjes, R.P., von Sicard, O., Pohle, R., Elen, B., Suriano, D., Pfister, V., Prato, M., Dipinto, S.,
8 Penza, M., 2016. Assessment of air quality microsensors versus reference methods: The
9 EuNetAir joint exercise. *Atmospheric Environment* 147, 246-263.
- 10 Castellini, S., Moroni, B., Cappelletti, D., 2014. PMetro: Measurement of urban aerosols on a
11 mobile platform. *Measurement* 49, 99-106.
- 12 Charron, A., Harrison, R.M., Moorcroft, S., Booker, J., 2004. Quantitative interpretation of
13 divergence between PM₁₀ and PM_{2.5} mass measurement by TEOM and gravimetric
14 (Partisol) instruments. *Atmospheric Environment* 38, 415-423.
- 15 de Nazelle, A., Bode, O., Orjuela, J.P., 2017. Comparison of air pollution exposures in active
16 vs. passive travel modes in European cities: A quantitative review. *Environment International*
17 99, 151-160.
- 18 Gao, M., Cao, J., Seto, E., 2015. A distributed network of low-cost continuous reading
19 sensors to measure spatiotemporal variations of PM_{2.5} in Xi'an, China. *Environmental*
20 *Pollution* 199, 56-65.
- 21 Grover, B.D., Eatough, N.L., Eatough, D.J., Chow, J.C., Watson, J.G., Ambs, J.L., Meyer,
22 M.B., Hopke, P.K., Al-Horr, R., Later, D.W., Wilson, W.E., 2006. Measurement of Both
23 Nonvolatile and Semi-Volatile Fractions of Fine Particulate Matter in Fresno, CA. *Aerosol*
24 *Science and Technology* 40, 811-826.
- 25 Gysel, M., Crosier, J., Topping, D.O., Whitehead, J.D., Bower, K.N., Cubison, M.J.,
26 Williams, P.I., Flynn, M.J., McFiggans, G.B., Coe, H., 2007. Closure study between chemical
27 composition and hygroscopic growth of aerosol particles during TORCH2. *Atmos. Chem.*
28 *Phys.* 7, 6131-6144.
- 29 Hagan, D., 2017. py-opc, <https://github.com/dhhagan/py-opc>.
- 30 Holstius, D.M., Pillarisetti, A., Smith, K.R., Seto, E., 2014. Field calibrations of a low-cost
31 aerosol sensor at a regulatory monitoring site in California. *Atmos. Meas. Tech.* 7, 1121-
32 1131.
- 33 Hu, D., Qiao, L., Chen, J., Ye, X., Yang, X., Cheng, T., Fang, W., 2010. Hygroscopicity of
34 inorganic aerosols: size and relative humidity effects on the growth factor. *Aerosol and Air*
35 *Quality Research* 10, 255-264.
- 36 Kumar, P., Morawska, L., Martani, C., Biskos, G., Neophytou, M., Di Sabatino, S., Bell, M.,
37 Norford, L., Britter, R., 2015. The rise of low-cost sensing for managing air pollution in
38 cities. *Environment International* 75, 199-205.
- 39 Lewis, A.C., Lee, J.D., Edwards, P.M., Shaw, M.D., Evans, M.J., Moller, S.J., Smith, K.R.,
40 Buckley, J.W., Ellis, M., Gillot, S.R., White, A., 2016. Evaluating the performance of low
41 cost chemical sensors for air pollution research. *Faraday Discussions* 189, 85-103.
- 42 Manikonda, A., Zíková, N., Hopke, P.K., Ferro, A.R., 2016. Laboratory assessment of low-
43 cost PM monitors. *Journal of Aerosol Science* 102, 29-40.
- 44 Mead, M.I., Popoola, O.A.M., Stewart, G.B., Landshoff, P., Calleja, M., Hayes, M., Baldovi,
45 J.J., McLeod, M.W., Hodgson, T.F., Dicks, J., Lewis, A., Cohen, J., Baron, R., Saffell, J.R.,
46 Jones, R.L., 2013. The use of electrochemical sensors for monitoring urban air quality in low-
47 cost, high-density networks. *Atmospheric Environment* 70, 186-203.



- 1 Mueller, M., Meyer, J., Hueglin, C., 2017. Design of an ozone and nitrogen dioxide sensor
- 2 unit and its long-term operation within a sensor network in the city of Zurich. Atmos. Meas.
- 3 Tech. Discuss. 2017, 1-29.
- 4 Petters, M., Kreidenweis, S., 2007. A single parameter representation of hygroscopic growth
- 5 and cloud condensation nucleus activity. Atmospheric Chemistry and Physics 7, 1961-1971.
- 6 Pope, F.D., 2010. Pollen grains are efficient cloud condensation nuclei. Environmental
- 7 Research Letters 5, 044015.
- 8 Pope, F.D., Dennis-Smith, B.J., Griffiths, P.T., Clegg, S.L., Cox, R.A., 2010. Studies of
- 9 single aerosol particles containing malonic acid, glutaric acid, and their mixtures with sodium
- 10 chloride. I. Hygroscopic growth. The Journal of Physical Chemistry A 114, 5335-5341.
- 11 Popoola, O.A.M., Stewart, G.B., Mead, M.I., Jones, R.L., 2016. Development of a baseline-
- 12 temperature correction methodology for electrochemical sensors and its implications for
- 13 long-term stability. Atmospheric Environment 147, 330-343.
- 14 Pöschl, U., 2005. Atmospheric aerosols: composition, transformation, climate and health
- 15 effects. Angewandte Chemie International Edition 44, 7520-7540.
- 16 Pringle, K.J., Tost, H., Pozzer, A., Pöschl, U., Lelieveld, J., 2010. Global distribution of the
- 17 effective aerosol hygroscopicity parameter for CCN activation. Atmos. Chem. Phys. 10,
- 18 5241-5255.
- 19 Rai, A., Kumar, P., Pilla, F., Skouloudis, A., Di Sabatino, S., Ratti, C., Yasar, A., Rickerby,
- 20 D., 2017. End-user Perspective of Low-cost Sensors for Outdoor Air Pollution Monitoring.
- 21 Science of The Total Environment.
- 22 Smith, K.R., Edwards, P., Evans, M.J., Lee, J.D., Shaw, M.D., Squires, F.A., Lewis, A.,
- 23 2017. Clustering approaches to improve the performance of low cost air pollution sensors.
- 24 Faraday Discussions, 1-15.
- 25 Snyder, E.G., Watkins, T.H., Solomon, P.A., Thoma, E.D., Williams, R.W., Hagler, G.S.W.,
- 26 Shelow, D., Hindin, D.A., Kilaru, V.J., Preuss, P.W., 2013. The Changing Paradigm of Air
- 27 Pollution Monitoring. Environmental Science & Technology 47, 11369-11377.
- 28 Sousan, S., Koehler, K., Hallett, L., Peters, T.M., 2016. Evaluation of the Alphasense optical
- 29 particle counter (OPC-N2) and the Grimm portable aerosol spectrometer (PAS-1.108).
- 30 Aerosol Science and Technology 50, 1352-1365.
- 31 Steinle, S., Reis, S., Sabel, C.E., Semple, S., Twigg, M.M., Braban, C.F., Leeson, S.R., Heal,
- 32 M.R., Harrison, D., Lin, C., Wu, H., 2015. Personal exposure monitoring of PM_{2.5} in indoor
- 33 and outdoor microenvironments. Science of The Total Environment 508, 383-394.
- 34 Viana, M., Rivas, I., Reche, C., Fonseca, A.S., Pérez, N., Querol, X., Alastuey, A., Álvarez-
- 35 Pedrerol, M., Sunyer, J., 2015. Field comparison of portable and stationary instruments for
- 36 outdoor urban air exposure assessments. Atmospheric Environment 123, 220-228.
- 37 Yin, J., Harrison, R.M., Chen, Q., Rutter, A., Schauer, J.J., 2010. Source apportionment of
- 38 fine particles at urban background and rural sites in the UK atmosphere. Atmospheric
- 39 Environment 44, 841-851.
- 40